CHAPTER VI

Impact of structural and morphological properties of rGONS/β-CD/ZnO nanocomposites on the electrochemical detection applications

CHAPTER VI

IMPACT OF STRUCTURAL AND MORPHOLOGIAL PROPERTIES OF rGONS/β-CD/ZnO NANOCOMPOSITES ON THE ELECTROCHEMICAL DETECTION APPLICATIONS

This chapter includes:

- Introduction
- Materials and methods
- Functional and Structural characterization of various concentrations of rGONS/β-CD/ZnO nanocomposite
- Morphological analysis
- Elemental analysis
- Electrocatalytic analysis for the sensing of nitrophenol isomers
- Conclusion
- References

6.1. INTRODUCTION

Electrochemical sensors based on the nanomaterials are highly focused on the current research field. Nanoparticles have unique physical and chemical properties that make them remarkably fit in the development of electrochemical sensors [1-5]. Various types of nanoparticles including metals, metal alloys, metal oxides, semiconductors and composites are employed in the development of advanced electrochemical sensors. Typically, the metal nanoparticles disclose great catalytic and conductivity properties. But for the detection of chemical species, semiconductor, transition metal oxides and non-transition metal oxide nanoparticles are typically employed as an electrode material [6-9]. In this present work, zinc oxide (ZnO) nanoparticles are used as an electrode modifying material.

ZnO nanoparticles belong to the class of metal oxide nanoparticles have received great attention due to its unique properties. These nanoparticles have a wide variety of applications in chemical sensors, UV-lasers, biosensors, gas sensors, UV-photodetectors, piezoelectric devices, dye-sensitized solar cells and transparent electronics [10-14]. The stability, high isoelectric point and powerful binding properties of zinc oxide nanoparticles make them a good electrode material in the development of advanced electrochemical sensors. The large surface to volume ratio is another advantage of employing ZnO as an auspicious electrode material for electrochemical sensing [15]. The zinc oxide nanoparticles with different morphology such as nanorods [16], nanopillar [17] nanowires [18] and nanorod-bundles [19] have already been employed for the electrode modification. In this present work, the ZnO nanoparticles with spindle like morphology are produced for the electrochemical sensing applications. The preparation of various types of ZnO nanostructures are based on different methods such as thermal evaporation [20], chemical solution deposition [21] and magnetron sputtering [22] etc. The facile wet chemical technique is employed for the synthesis of spindle like zinc oxide nanoparticles along with the reduced graphene oxide nanosheet (rGONS) and β-cyclodextrin (β-CD) polymer and employed as an electrode modifying materials for the electrochemical detection of nitrophenol isomers. The objective of this work is to synthesize a morphology controlled zinc oxide nanoparticles decorated β-cyclodextrin functionalized reduced graphene oxide nanosheets for the effective detection of nitrophenol isomers by electrochemical method.

6.2. MATERIALS AND METHODS

Graphene oxide (GO) nanosheets are synthesized using purified natural graphite powder via modified Hummer's method [23]. The β-cyclodextrin polymer (β-CD) functionalized reduced graphene oxide nanosheets (rGONS/β-CD) are synthesized by taking dispersed solution of 50 mg of graphene oxide (GO) and 2 mg/ml of β-cyclodextrin polymer. The β-CD polymer is added dropwise into the dispersed graphene oxide suspension followed by the addition of hydrazine hydrate as a reducing agent and stirred for 4 hours at 60˚C [24-25]. The reaction mixture is then centrifuged and dispersed in an aqueous medium for the embellishment of zinc oxide nanoparticles. 0.002 M of zinc acetate dihydrate ($C_4H_6O_4Zn.2H_2O$) is dispersed in 100 ml of deionized water and added into the dispersed rGONS/β-CD suspension followed by the addition

of 0.005 M of sodium borohydrate ($NaBH_4$) as a reducing agent and stirred for 4 hours at 80˚C. The reaction mixture is then centrifuged using double distilled water and dried at 60˚C for 4 hours [23] [26]. Similarly 0.004 M, 0.006 M, 0.008 M and 0.01 M of zinc oxide nanoparticles embellished β-cyclodextrin functionalized reduced graphene oxide nanosheets (rGONS/β-CD/ZnO) are synthesized.

6.3. RESULTS AND DISCUSSION

6.3.1. FT-IR SPECTRAL ANALYSIS

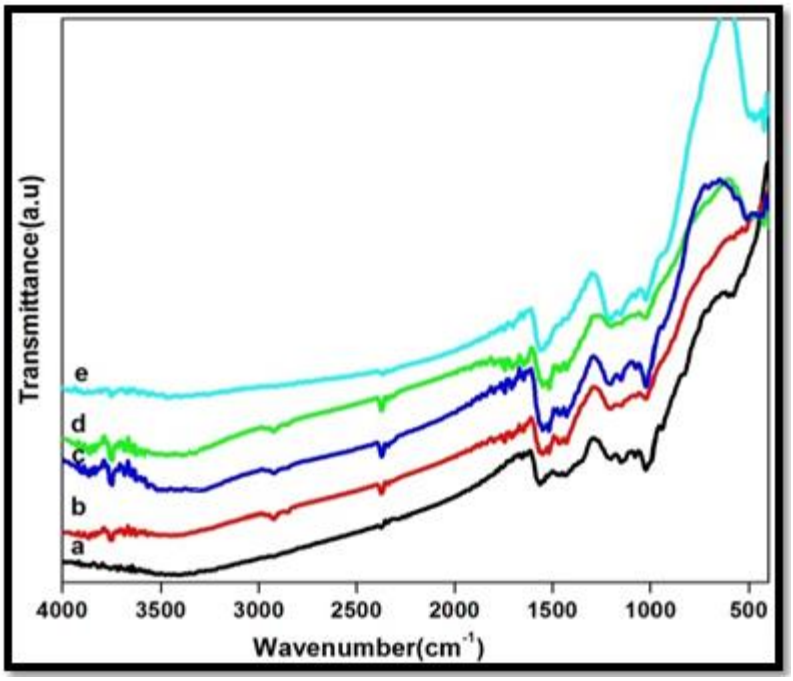

Figure.6.1. FT-IR spectra of zinc oxide nanoparticles embellished β-cyclodextrin functionalized reduced graphene oxide nanosheets using (a) 0.002 M (b) 0.004 M (c) 0.006 M (d) 0.008 M and (e) 0.01 M molar ratios of zinc acetate dihydrate

The FT-IR spectra of zinc oxide nanoparticles embellished β-cyclodextrin functionalized reduced graphene oxide nanosheets (rGONS/β-CD/ZnO) synthesized using various molar ratios (0.002 M, 0.004 M, 0.006 M, 0.008 M and 0.01 M) of zinc acetate dihydrate is shown in the Figure.6.1.(a-e). The formation of reduced graphene oxide nanosheets in all the five molar ratios of synthesized rGONS/β-CD/ZnO nanocomposites are confirmed by observing the absorption bands of carbon-oxygen functional groups such as O-H stretching, unoxidized C=C stretching and C-O stretching (epoxy) at 3485.1 cm^{-1} 1585.4 cm^{-1} and 1231 cm^{-1} respectively.The absence

of absorption peak at 1740 cm^{-1} corresponds to the C=O carboxyl functional group confirms the reduction of graphene oxide into the reduced graphene oxide nanosheets [23]. The presence of chemically functionalized β-cyclodextrin polymer in the synthesized rGONS/β-CD/ZnO nanocomposite is identified by observing the absorption bands of O-H stretching, C-H_2, C-H, C-O (carboxy), and O-H functional groups at 3752 cm^{-1}, 2924.62 cm^{-1}, 2373.41 cm^{-1}, 1430.21 cm^{-1} and 1023 cm^{-1} respectively [24-28].

The characteristic bands observed between 400 to 700 cm^{-1} may corresponds to the zinc oxide (Zn-O) nanoparticles embellished on the surface of rGO/β-CD nanosheets [29-30]. The embellishment of zinc oxide nanoparticles on the surface of rGO/β-CD nanosheets in the synthesized nanocomposite is confirmed by the gradual decrease in the depth of the absorption bands of oxygen containing functional groups such as O-H, C=C, C-O and C-H of rGONS and β-CD polymer with the increase in the molar ratio of zinc acetate dihydrate from 0.002 M to 0.01 M. This may be due to the increase in the interlayer distance of rGO nanosheets by the inclusion of ZnO nanoparticles to the adjacent layers of rGO/β-CD nanosheets. It is observed from the FT-IR spectra of various molar ratios of rGONS/β-CD/ZnO nanocomposite that the band depth of zinc oxide nanoparticles increases with the increase in the molar ratio of zinc acetate dihydrate from 0.002 M to 0.01 M, which further confirms the uniform embellishment and increase in the zinc oxide nanoparticles concentration on the rGONS/β-CD surface and this could also be evidenced from SEM and EDAX analysis [31].

6.3.2. STRUCTURAL ANALYSIS

The XRD pattern of zinc oxide nanoparticles embellished β-cyclodextrin functionalized reduced graphene oxide nanosheets (rGONS/β-CD/ZnO) synthesized using 0.002 M, 0.004 M, 0.006 M, 0.008 M and 0.01 M molar ratio of zinc acetate dihydrate is shown in the Figure.6.2.(a-e). The diffraction peaks of zinc oxide nanoparticles observed at 31.7˚, 34.6˚, 36.4˚, 47.5˚, 56.7˚, 62.9˚ and 67.9˚ confirms the formation of (100), (002), (101), (102), (110), (103) and (112) crystalline planes of wurtzite hexagonal structure of zinc oxide nanoparticles in the rGONS/β-CD/ZnO nanocomposite respectively and the diffraction patterns are in agreement with the standard JCPDS card. No 36-1451 [14] [29] [32]].

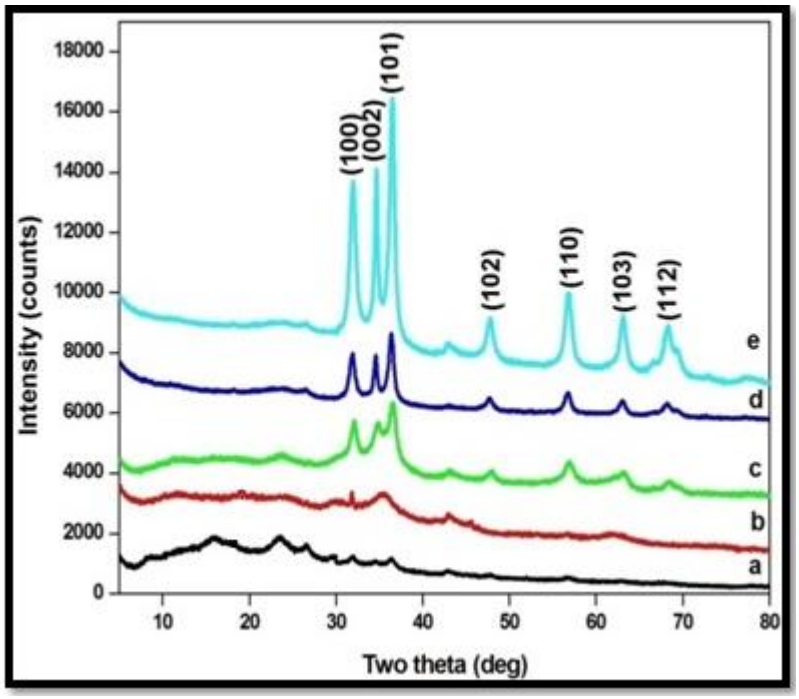

Figure.6.2. XRD spectra of zinc oxide nanoparticles embellished β-cyclodextrin functionalized reduced graphene oxide nanosheets using (a) 0.002 M (b) 0.004 M (c) 0.006 M (d) 0.008 M (e) 0.01 M molar ratio of zinc acetate dihydrate

The complete disappearance of typical (002) diffraction peak of graphene oxide nanosheets (as discussed in the chapter 3) and the appearance of broad diffraction peak at 23.2˚ confirms the reduction of graphene oxide nanosheets into reduced graphene oxide nanosheets during the functionalization of β-cyclodextrin polymer with the GO nanosheets [32]. Using the Debye Scherrer's formula [14], the crystallite size (D) of the zinc oxide nanoparticles embellished on the surface of rGO/β-CD nanosheets are calculated from full width half maxima (FWHM) of XRD peaks. The calculated crystallite size values of zinc oxide nanoparticles synthesized using various molar ratios (0.002 M, 0.004 M, 0.006 M, 0.008 M and 0.01 M) of zinc acetate dihydrate are found to be 24.21 nm, 22.69 nm, 21.71 nm, 19.85 nm and 27.99 nm, respectively.

The broad diffraction peak of rGONS/β-CD is observed only for the rGONS/β-CD/ZnO nanocomposite synthesized for lower molar ratios (0.002 M, 0.004 M and 0.006 M) of zinc acetate dihydrate and this confirms the embellishment of small amount of ZnO nanoparticles on the rGONS/β-CD surface [31]. The broadening in the diffraction peak of rGONS/β-CD may be attributed to the cross-linking formation of β-CD polymer with graphene oxide nanosheets that reduces the crystalline nature of

graphene oxide nanosheets and β-CD polymer. This amorphous nature of rGONS/β-CD improves the surface to volume ratio of rGONS/β-CD/ZnO nanocomposites that makes the β-CD polymer chain more flexible and results in the enhancement of ionic conductivity and the adsorption amount of zinc oxide nanoparticles on the surface of rGO/β-CD nanosheets [33]. The diffraction peak of carbon atoms in reduced graphene oxide nanosheets is not observed for the higher molar ratios of (0.006 M to 0.01 M) rGONS/β-CD/ZnO nanocomposite. This may be due to the large amount of well crystalline zinc oxide nanoparticles embellished on the surface of rGONS/β-CD that weakens the diffraction of carbon atoms [31]. Relatively, the diffraction peaks intensity of zinc oxide nanoparticles on the rGONS/β-CD surface increases with the increase in the zinc acetate dihydrate molar ratio from 0.002 M to 0.01 M. This may be due to the polydirectional arrangement of zinc oxide nanoparticles on the rGONS/β-CD surface [32]. Hence, it is revealed from the XRD analysis that the rGONS/β-CD/ZnO nanocomposite synthesized using 0.008 M molar ratio of zinc acetate dihydrate has smaller crystallite size for ZnO nanoparticles on the rGONS/β-CD surface, which could provide a significant effect on the electrochemical sensing of nitrophenol isomers.

6.3.3. SEM ANALYSIS

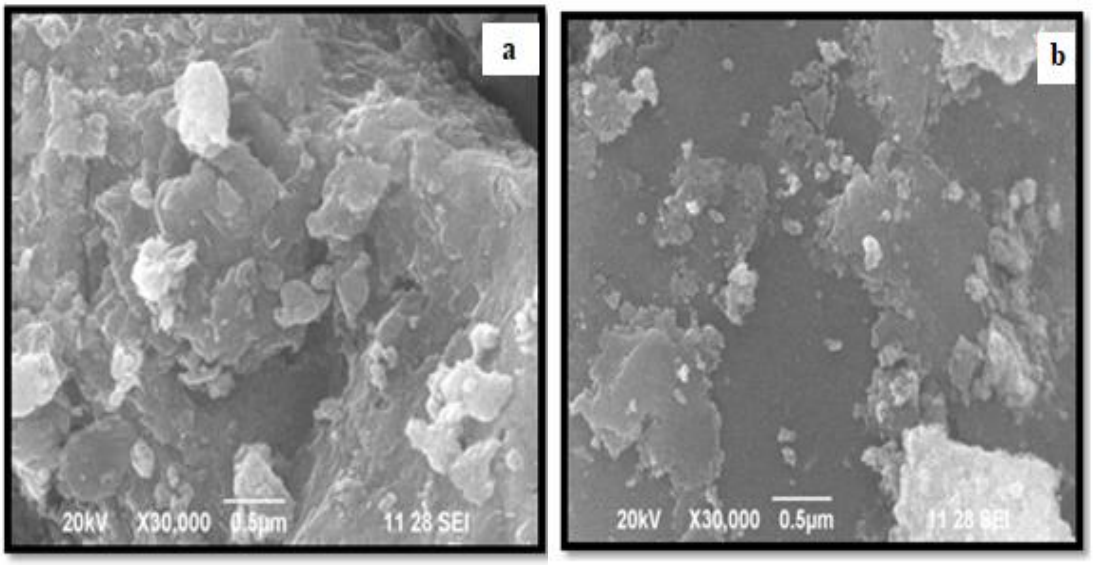

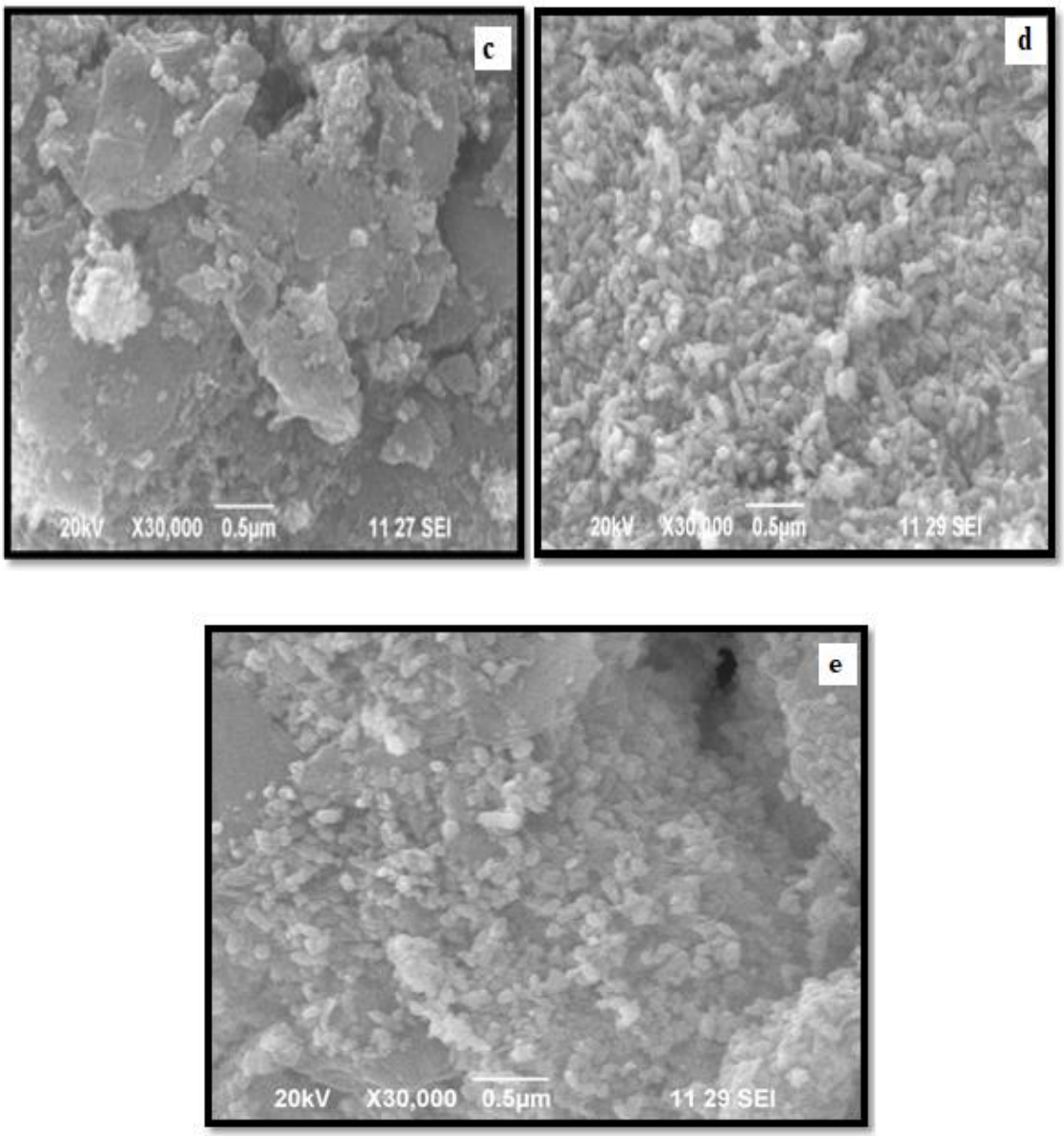

Figure.6.3. SEM images of zinc oxide nanoparticles embellished β-cyclodextrin functionalized reduced graphene oxide nanosheets using (a) 0.002 M (b) 0.004 M (c) 0.006 M (d) 0.008 M and (e) 0.01 M molar ratio of zinc acetate dihydrate

Scanning electron microscope is a significant instrumental technique to characterize and investigate the microstructure and morphological surface of the materials. Scanning electron micrograph of the surface and cross section of zinc oxide nanoparticles embellished β-cyclodextrin functionalized reduced graphene oxide nanosheets (rGONS/β-CD/ZnO) synthesized using various molar ratios (0.002 M, 0.004 M, 0.006 M, 0.008 M and 0.01 M) of zinc acetate dihydrate is shown in the Figure.6.3.(a-e). The SEM images of the lower concentrations of (0.002 M and

0.004 M) rGONS/β-CD/ZnO nanocomposite clearly depicts the formation of layer structured reduced graphene oxide nanosheets in the form of wrinkled and crumpled paper like sheets which may be attributed to the functionalization of β-cyclodextrin polymer with the rGO nanosheets and these results are in consistent with the SEM images of rGO/β-CD nanosheets as discussed in the chapter 3 [29]. This may enhance the large surface area of rGO nanosheets for the embellishment of zinc oxide nanoparticles, thereby enhancing the adsorption amount of nitrophenol isomer sites on the electrode surface [32]. The uniform embellishment of large amount of zinc oxide nanoparticles is observed with the continuous increase in the molar of zinc acetate dihydrate from 0.006 M to 0.008 M. With the further increase in the molar ratio of zinc acetate dihydrate above 0.008 M, the SEM image of rGONS/β-CD/ZnO nanocomposite shows the wrinkled rGO/β-CD nanosheets with agglomerated zinc oxide nanoparticles.

The SEM images of rGONS/β-CD/ZnO shows the spindle like morphology of ZnO nanoparticles with agglomeration for the molar ratio of 0.01 M of zinc acetate dihydrate which may be due to the presence of more number of Zn^{2+} ions in the reaction system. With the continuous reduction in the molar ratio of zinc acetate dihydrate from 0.01 M to 0.004 M, the amount of Zn^{2+} ions in the reaction system is sufficient to produce smaller size spindle-like zinc oxide nanoparticles without agglomeration (Figure.6.3 (b, c and d)). With the further reduction in the molar ratio of zinc acetate dihydrate into 0.002 M, the spindle-like morphology of zinc oxide nanoparticles is not evident and this may be due to the insufficient amount of Zn^{2+} ions. This may also be due to the predominance of β-cyclodextrin polymer and also the layered structure of reduced graphene oxide nanosheets [32]. The SEM analysis also revealed that the amount of zinc oxide nanoparticles embellished on the surface of rGO/β-CD nanosheets are found to be increase gradually with the increase in the molar ratio of zinc acetate dihydrate from 0.002 M to 0.01 M.

The role of reduced graphene oxide nanosheets, β-cyclodextrin polymer as a surfactant, the molar ratio of zinc acetate dihydrate on the size, morphology, dispersion and the electrochemical stability of rGONS/β-CD/ZnO nanocomposites are evidenced from the morphological investigation on the smaller sized and spindle like zinc oxide nanoparticles embellished rGONS/β-CD nanocomposites [32]. It is further evidenced that the rGONS/β-CD/ZnO nanocomposite synthesized using 0.008 M molar ratio of

zinc acetate dihydrate shows the large amount of spindle-like zinc oxide nanoparticles embellished β-cyclodextrin functionalized reduced graphene oxide nanosheets and that could show the significant effect on the electrochemical sensing of nitrophenol isomers.

6.3.4. EDAX ANALYSIS

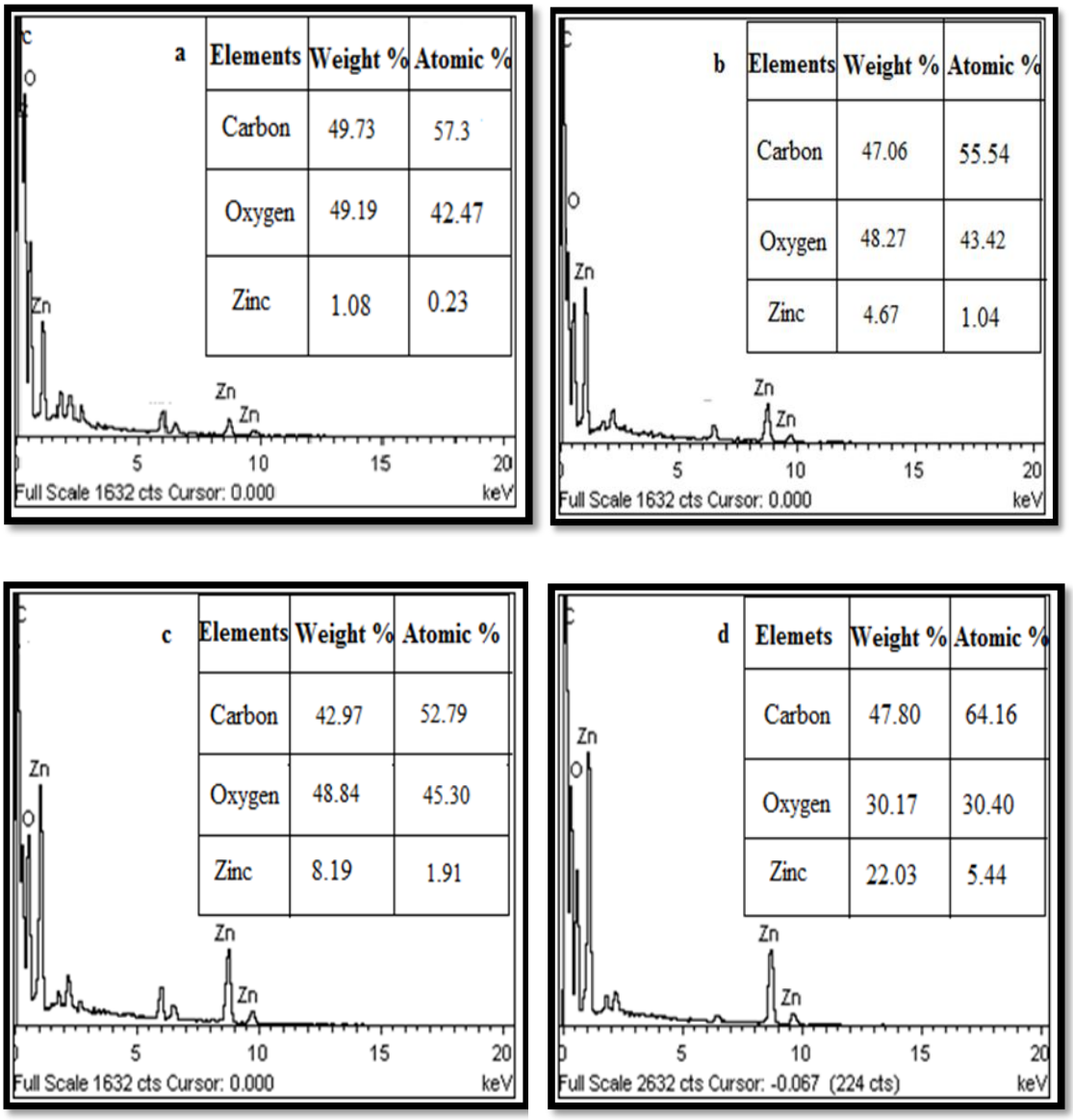

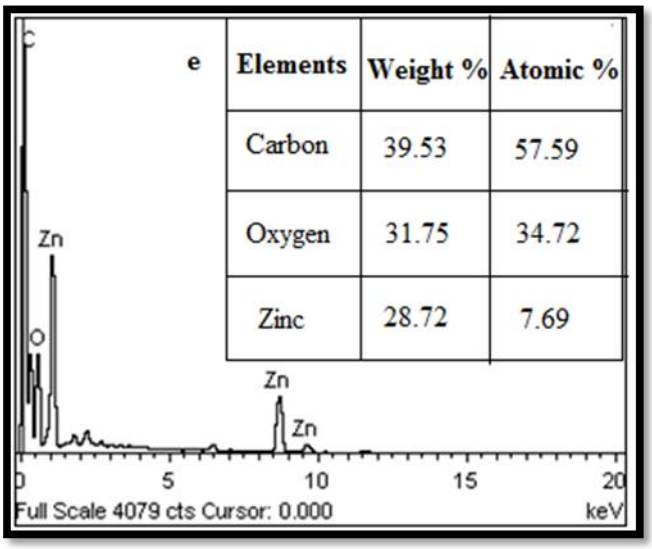

Figure.6.4. EDAX spectra of zinc oxide nanoparticles embellished β-cyclodextrin functionalized reduced graphene oxide nanosheets using (a) 0.002 M (b) 0.004 M (c) 0.006 M (d) 0.008 M and (e) 0.01 M molar ratios of zinc acetate dihydrate

The synthesized 0.002 M, 0.004 M, 0.006 M, 0.008 M and 0.01 M molar ratios of rGONS/β-CD/ZnO nanocomposite is subjected to energy dispersive X-ray (EDAX) analysis in order to confirm the chemical composition of the samples and are shown in the Figure.6.4.(a-e). EDAX images of various molar ratios of synthesized rGONS/ β-CD/ZnO nanocomposites clearly show the elemental peaks corresponding to carbon, oxygen and zinc without any elemental impurities. The atomic and weight percentage of elements present in the synthesized rGONS/β-CD/ZnO nanocomposite is shown in the inset of the Figure.6.4.(a-e). The EDAX result confirms the formation of zinc oxide nanoparticles decorated β-cyclodextrin functionalized reduced graphene oxide nanosheets without any impurities [34].

6.3.5. HRTEM ANALYSIS

The structural, morphological and elemental investigation reveals that the rGONS/β-CD/ZnO nanocomposite synthesized using 0.008 M concentration of zinc acetate dihydrate shows the smaller crystallite size and controlled morphology without agglomeration and hence it is further characterized using High resolution transmission electron microscope (TEM) analysis.

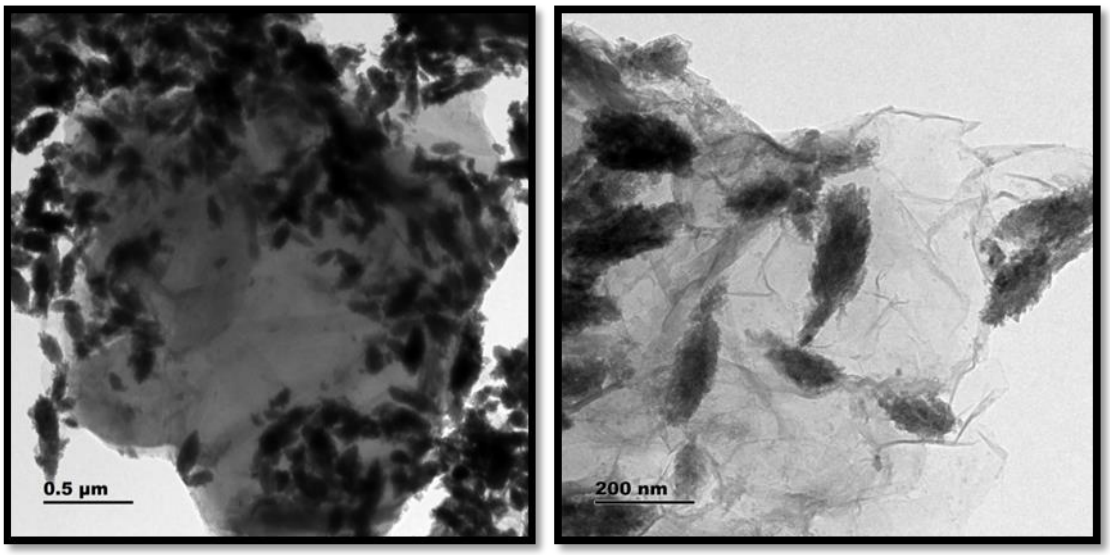

Figure.6.5. TEM images of zinc oxide nanoparticles embellished β-cyclodextrin functionalized reduced graphene oxide nanosheets using 0.008 M molar ratio of zinc acetate dihydrate

The particle size, morphology and the distribution of 0.008 M molar ratio of synthesized rGONS/β-CD/ZnO nanocomposite is examined using a high resolution transmission electron microscope (HRTEM) and the results are shown in the Figure.6.5 [35]. It is observed that the wrinkled structure morphology of β-cyclodextrin functionalized reduced graphene oxide nanosheets are uniformly embellished with zinc oxide nanoparticles [36]. The formation of reduced graphene oxide nanosheets with high surface area and wrinkled morphology confirms the strong π-π interaction between β-cyclodextrin polymer and reduced graphene oxide nanosheets. This polymer functionalized reduced graphene oxide nanosheets acts as a good surface for the growth of zinc oxide nanoparticles with controlled morphology [37]. It is also observed that the zinc oxide nanoparticles embellished on the surface of rGO/β-CD nanosheets shows the spindle shaped and are uniformly distributed without any agglomeration [38]. The uniformly embellished spindle shape zinc oxide nanoparticles may effectively block the hole penetration, thereby decreases the recombination of charge carriers between the interfacial layers. This may enhance the excellent electrical property of the synthesized rGONS/β-CD/ZnO nanocomposites [29] [37]. The observed HRTEM results are in consistent with the XRD and SEM results. It is further confirmed from the TEM analysis that the rGO/β-CD nanosheets are good supporting material for the embellishment of ZnO nanoparticles and also the synthesized nanocomposites are good

electrode surface modifying material for the electrochemical detection of nitrophenol isomers [34].

6.3.6. SAED ANALYSIS

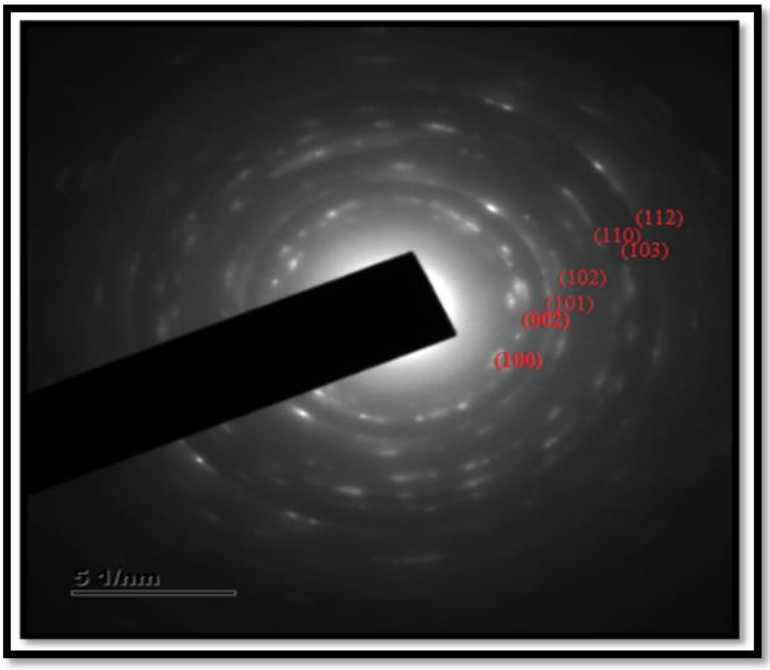

Figure.6.6. SAED pattern of zinc oxide nanoparticles embellished β-cyclodextrin functionalized reduced graphene oxide nanosheets using 0.008 M molar ratio of zinc acetate dihydrate

The selected area electron diffraction (SAED) pattern of synthesized 0.008 M molar ratio of zinc oxide nanoparticles embellished β-cyclodextrin functionalized reduced graphene oxide nanosheets is shown in the Figure.6.6. It gives the deeper insight into the crystallographic structure of synthesized rGONS/β-CD/ZnO nanocomposites [37]. The rings obtained in SAED pattern of the synthesized rGONS/ β-CD/ZnO nanocomposite confirms the crystalline nature of the zinc oxide nanoparticles embellished on the surface of rGONS/β-CD nanosheets. The obtained SAED pattern is well matched with the (111), (002), (101), (102), (103), (110) and (112) crystalline planes of wurzite structure of zinc oxide nanoparticles embellished on the rGO/β-CD nanosheets which is in consistent with the XRD analysis [29].

6.4. ELECTROCHEMICAL BEHAVIOUR OF MODIFIED ELCTRODES

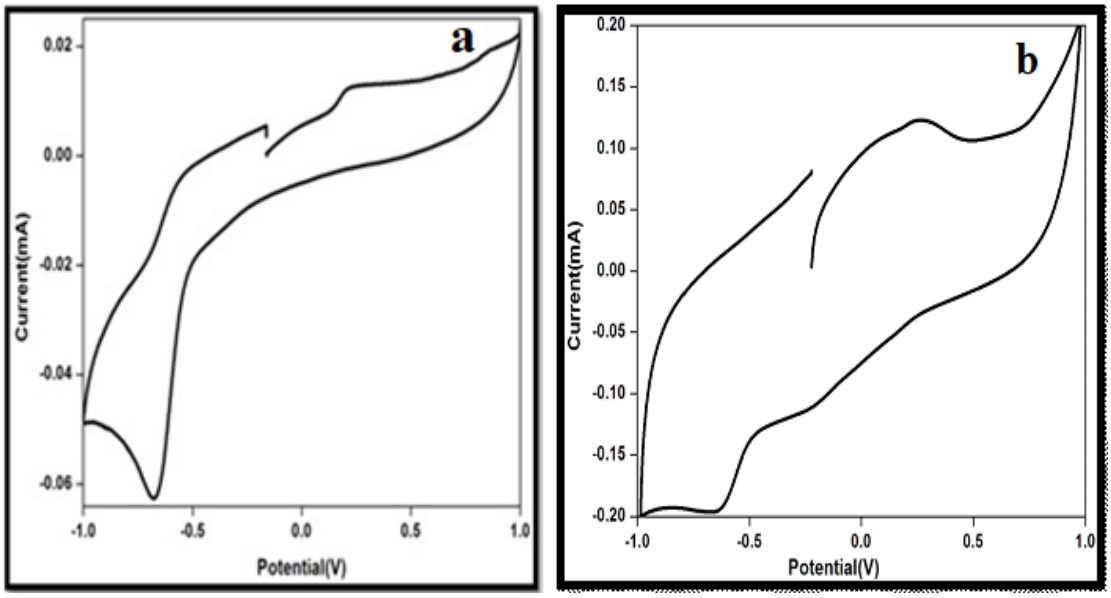

Figure.6.7. Cyclic voltagramm of 220 µM of o-NP at the (a) rGONS/ZnO/GCE (b) rGONS/β-CD/ZnO/GCE in PBS solution at the scan rate of 10 mV/s

To study the electrochemical performance of various modified electrodes such as rGONS/ZnO/GCE and rGONS/CD/ZnO/GCE, the concentration of ortho-nitrophenol in the PBS electrolyte medium is varied from 100 to 230 µM and 20 to 230 µM respectively and the maximum redox peak current is observed for the 220 µM of ortho-nitrophenol. Figure.6.7.(a and b) shows the cyclic voltammetric responses of 220 µM of ortho-nitrophenol for zinc oxide nanoparticles embellished reduced graphene oxide nanosheets modified glassy carbon electrode (GCE) (rGONS/ZnO/GCE) and zinc oxide nanoparticles embellished β-cyclodextrin functionalized reduced graphene oxide nanosheets modified GCE (rGONS/β-CD/ZnO/GCE) in 0.1 M of phosphate buffer solution (PBS) at the scan rate of 10 mVs^{-1} within the potential range from -1 V to +1 V. It shows the well defined reversible redox peaks with the reduction and oxidation peak potentials at -0.7 V, +0.24 V and with the cathodic and anodic peak current of -0.061 mA, +0.011 mA, and -0.21, +0.13 mA for rGONS/ZnO/GCE and rGONS/ β-CD/ZnO/GCE respectively. It is observed that the electrocatalytic performance of rGONS/β-CD/ZnO nanocomposite modified GCE towards the detection of 220 µM ortho-nitrophenol is much higher than the rGONS/ZnO/GCE, thereby confirms the impact of β-cyclodextrin polymer in the enhancement of electrocatalytic property of

rGONS/β-CD/ZnO nanocomposite [39]. The chemical functionalization of β-cyclodextrin polymer with the rGO nanosheets enhances the surface area and electrical conductivity of rGONS, thereby enhances the adsorption amount of o-NP sites. It also enhances the acceleration rate of electron transfer between the electrode surface and ortho-nitrophenol sites, which generates the significant microenvironment for the electrocatalytic detection of ortho-nitrophenol. The electrocatalytic response of rGONS/β-CD/ZnO/GCE towards the detection of ortho-nitrophenol is also found to be higher in comparison with that of rGONS/β-CD/GCE (as discussed in the chapter 3). Hence, the glassy carbon electrode modified using rGONS/β-CD/ZnO nanocomposite is a better choice for the electrochemical detection of nitrophenol isomers.

6.5. ELECTROCHEMICAL DETECTION OF NITROPHENOL ISOMERS

The various molar ratios of synthesized rGONS/β-CD/ZnO nanocomposite is employed for the effective electrochemical detection of nitrophenol isomers such as ortho-, para-and meta-nitrophenol. The maximum electrochemical detection ability of rGONS/β-CD/ZnO nanocomposite towards the detection of nitrophenol isomers could be achieved by optimizing the parameters such as concentration of zinc oxide nanoparticles on the surface of rGO/β-CD nanosheets, pH of the phosphate buffer solution and scan rate of the redox reactions and the results are presented.

6.5.1. Effect of rGONS/β-CD/ZnO concentration on electrocatalytic activity

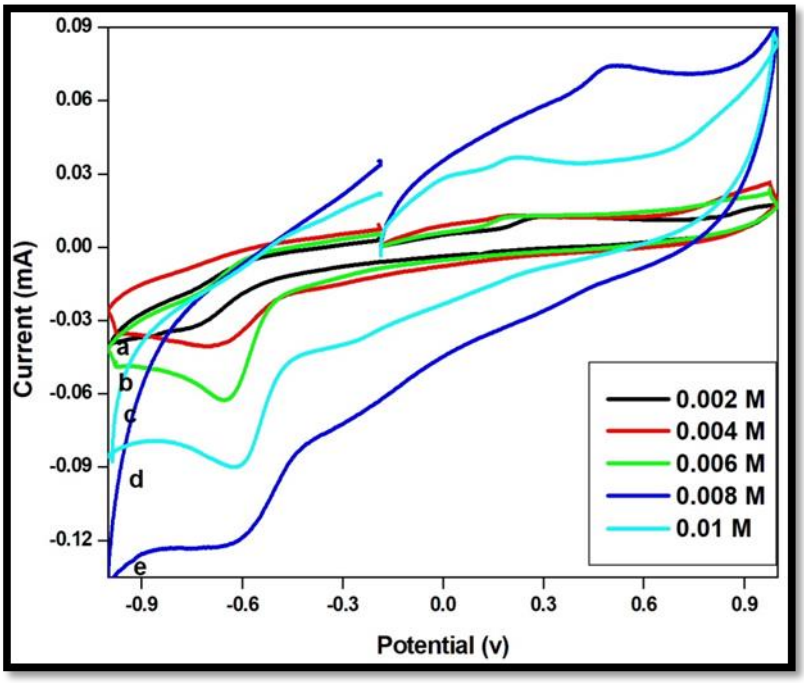

Figure.6.8. Cyclic voltagramm of 220 µm of o-NP at (a) 0.002 M (b) 0.004 M (c) 0.006 M (d) 0.008 M and (e) 0.01 M zinc oxide nanoparticles embellished β-cyclodextrin functionalized reduced graphene oxide nanosheets in PBS solution

The maximum electrocatalytic activity of ortho-nitrophenol at rGONS/β-CD/ZnO nanocomposite modified GCE could be studied by the effect of different molar ratios (0.002 M, 0.004 M, 0.006 M, 0.008 M and 0.01 M) of zinc oxide nanoparticles embellished β-cyclodextrin functionalized reduced graphene oxide nanosheets in 0.1 M of phosphate buffer solution (PBS) containing 220 µM of o-NP at the scan rate of 10 mV/s and the results are shown in the Figure.6.8.(a-e). It is observed from the Figure.6.8.(a-e) that the gradual increase in the molar ratio of zinc acetate dihydrate from 0.002 M to 0.008 M enhances the redox peak current of o-NP [40] and may be due to the formation of large amount of spindle like morphology of zinc oxide nanoparticles without agglomeration, which could also be evidenced from SEM analysis. With the further increase in the molar ratio of zinc acetate dihydrate into 0.01 M, the electrocatalytic redox peak current for 220 µM of o-NP is decreased and may be due to the embellishment of large number of zinc oxide nanoparticles on the surface of rGO/β-CD nanosheets that leads to agglomeration, thereby decreases the electrochemical

sensing property of nanocomposite which could also be evidenced from SEM analysis [41].

The maximum redox peak current of o-NP is observed for the 0.008 M molar ratio of rGONS/β-CD/ZnO modified GCE. This implies that the zinc oxide nanoparticles with high molar ratio, good morphology and smaller crystallite size could improve the specific surface area of rGONS/β-CD/ZnO nanocomposite for the accumulation of large amount of ortho-nitrophenol, thereby improves the electrochemical reaction of o-NP on the modified electrode surface [42]. It is also evident that the rGONS/β-CD/ZnO nanocomposite with agglomerated zinc oxide nanoparticles shows the decrease in the current response, even though the concentration of zinc oxide nanoparticles is larger [42]. Hence, the 0.008 M molar ratio of rGONS/β-CD/ZnO modified GCE is employed for the detection of all three nitrophenol isomers.

6.5.2 Effect of electrolyte pH

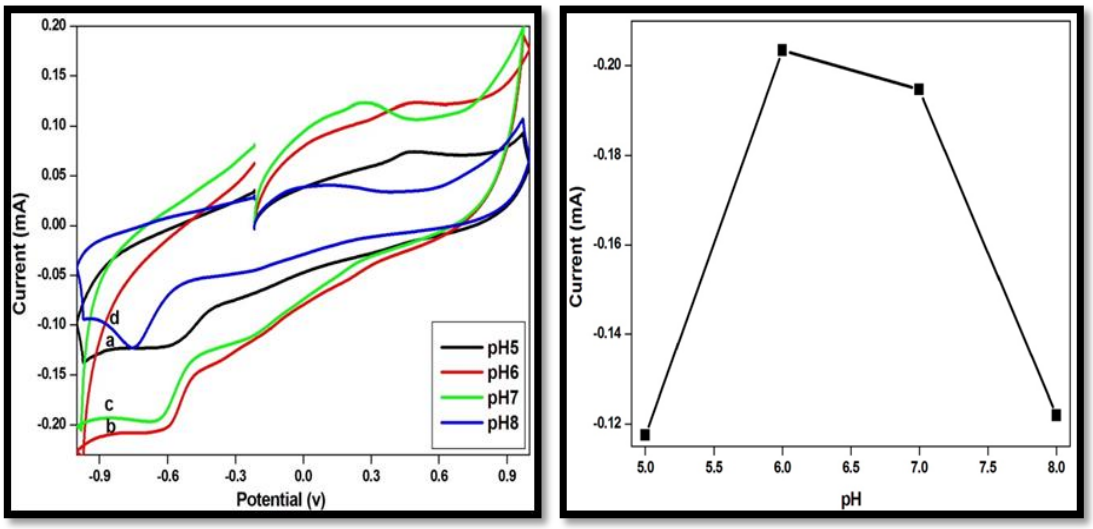

(a)

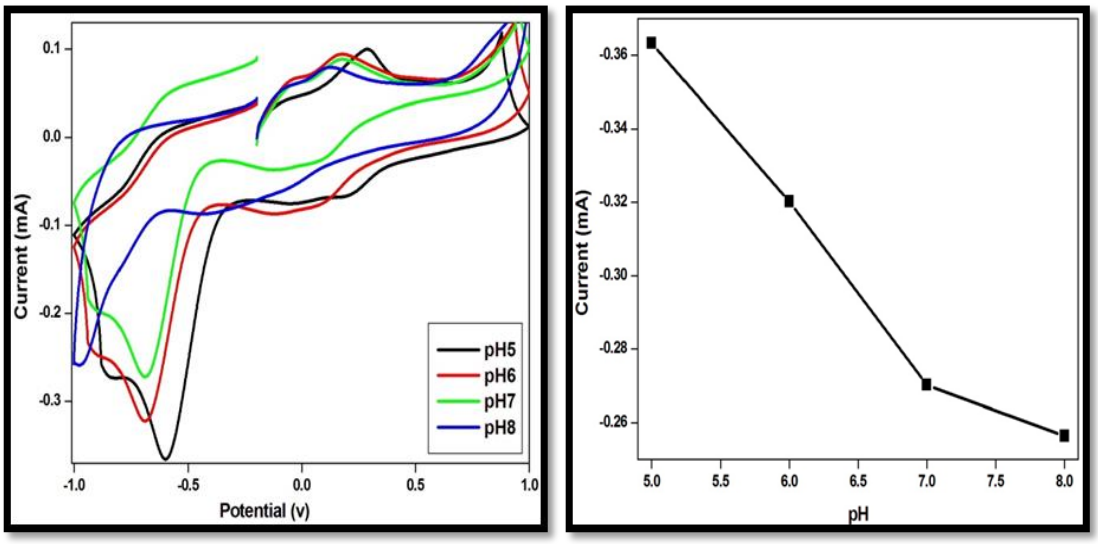

(b)

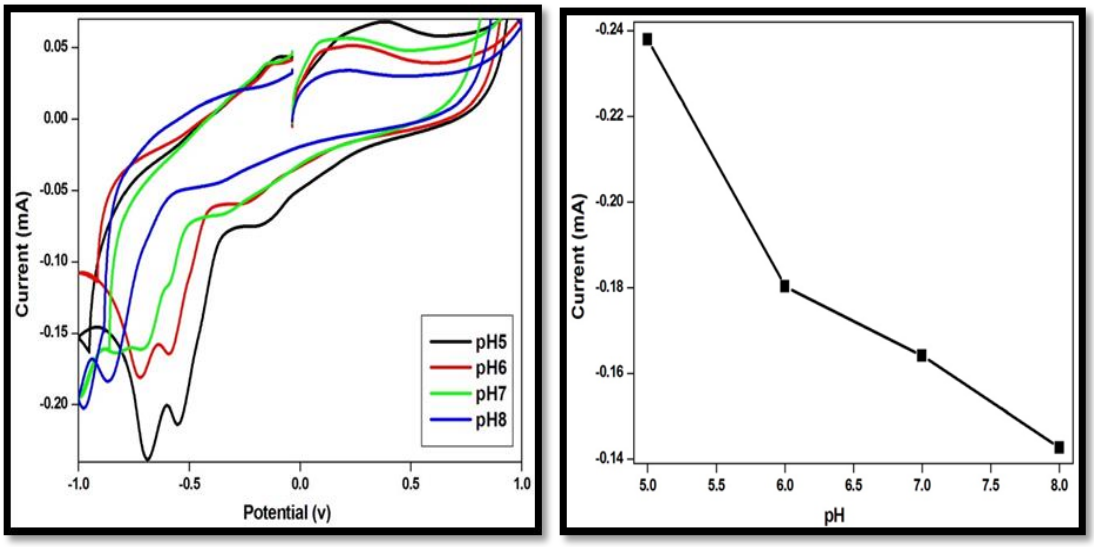

(c)

Figure.6.9. Effects of pH on the reduction peak current of (a) 220 µM o-NP and its linearity (b) 240 µM p-NP and its linearity (c) 240 µM m-NP and its linearity in 0.1 M of PBS solution at the scan rate of 10 mV/s

The influence of pH on the electrocatalytic performance of 220 µm of ortho-, 240 µm of para- and 240 µm of meta-nitrophenol isomers at the 0.008 M molar ratio of rGONS/β-CD/ZnO modified GCE surface is investigated using cyclic voltammetry in PBS solution with the pH range from 5.0 to 8.0 at the scan rate of 10 mV/s. It is evident from the Figure.6.9.(a-c) that the redox peak potential and current

intensities strongly depends on the pH value of the phosphate buffer solution. It is observed from the Figure.6.9.(a-c) that, with the increase of pH from 5.0 to 8.0, the reduction peak potential corresponds to the ortho-, para- and meta-nitrophenol isomers linearly shifted more towards the negative values thereby indicating that the protons are directly involved in the electrocatalytic redox process [42] [43].

It is also observed from the calibration graph (Figure.6.9.(a)) for pH dependent that the redox peak current of ortho-nitrophenol increases gradually with the increase in the pH value from 5.0 to 6.0 and the maximum redox peak current is obtained for the pH of 6.0. With the further increase in the pH from 6.0 to 8.0, the electrocatalytic redox peak current of ortho-nitrophenol decreases [41-42]. But, in the calibration graph (Figure.6.9.(b and c)) for the redox peak current of para- and meta-nitrophenol isomers increases initially for the pH of 5.0 and with the continuous increase in the pH of the PBS solution to 6.0 to 8.0, the redox peak current decreases [41-42]. The pH dependency may be attributed to the concentration of protons, that plays a significant role in the electrocatalytic reaction, as the electrolyte medium with high pH values decreases the proton concentration, which thereby reduces the electrocatalytic redox reaction and also the pH of the electrolyte medium affects the detection of microenvironment, which in turn affect the inclusion complexes ability of ortho-, para- and meta-nitrophenol sites [41]. Hence, the phosphate buffer solution with the pH of 6.0, 5.0 and 5.0 is chosen as a supporting electrolyte medium for the further electrocatalytic investigation of ortho-, para-and meta-nitrophenol isomers respectively.

6.5.3. Effect of scan rate

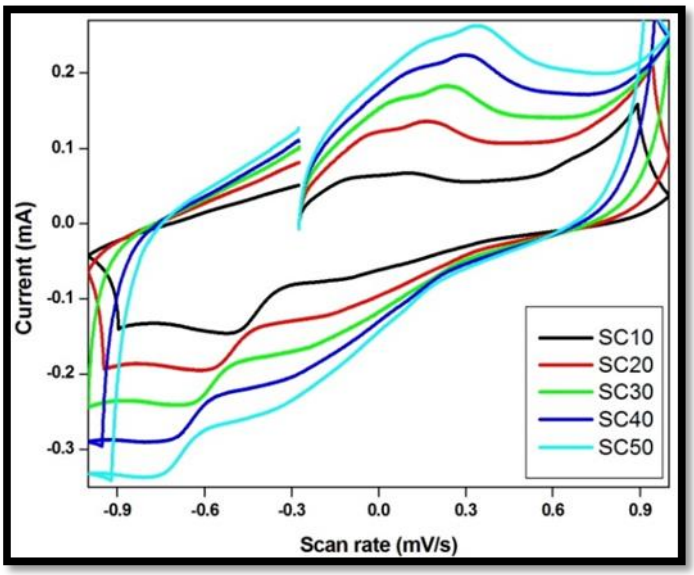

(a)

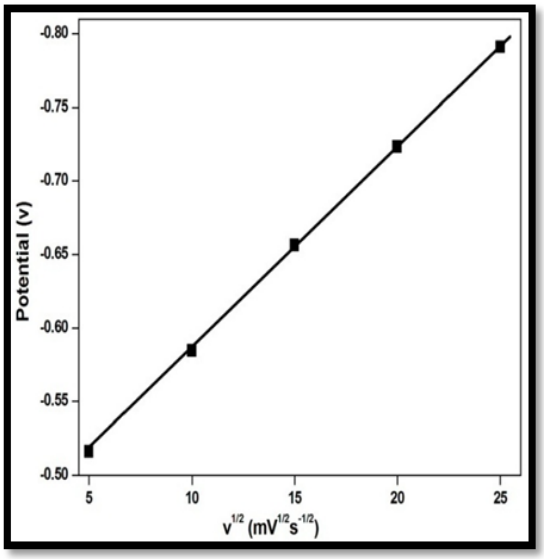

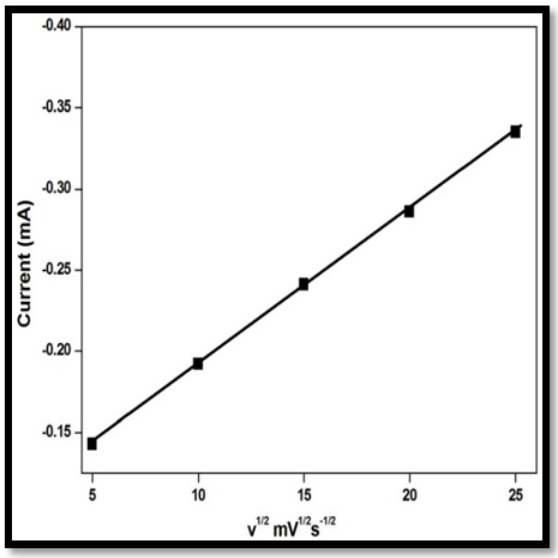

(b)

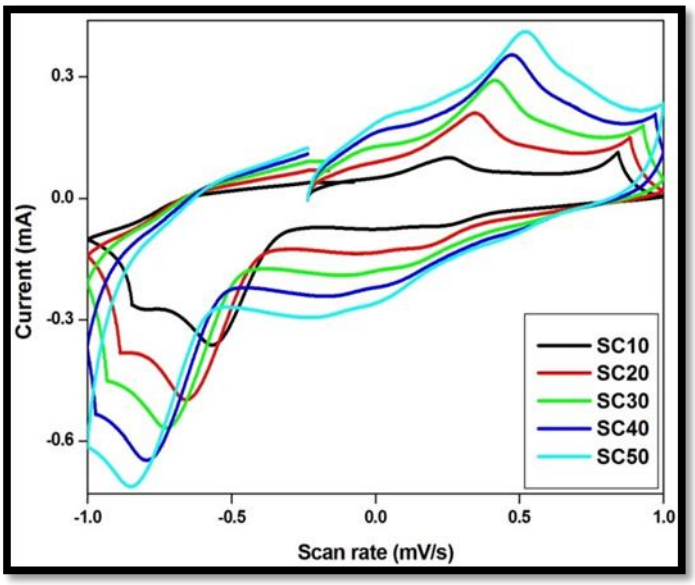
Current (mA)
Scan rate (mV/s)
SC10
SC20
SC30
SC40
SC50

(c)

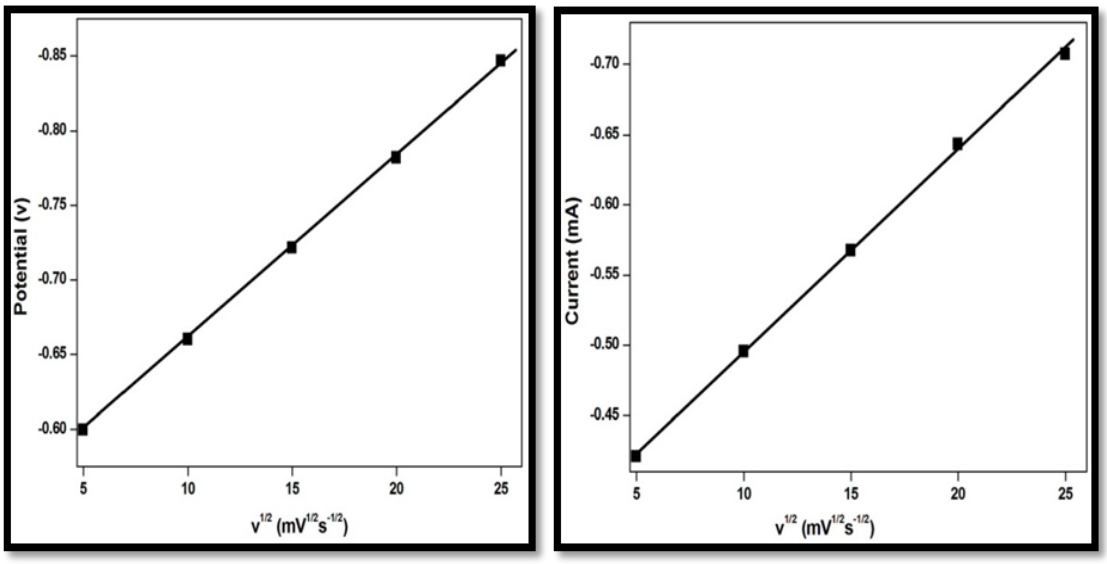
Potential (v)
v^1/2 (mV^1/2s^-1/2)
Current (mA)
v^1/2 (mV^1/2s^-1/2)

(d)

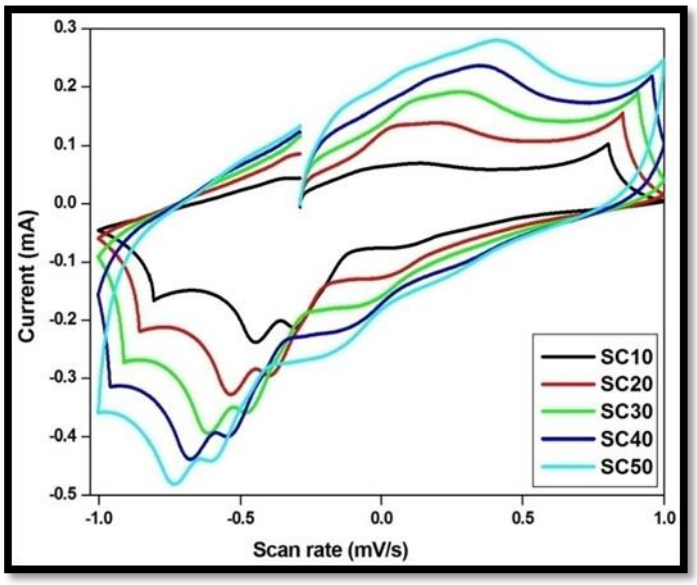

(e)

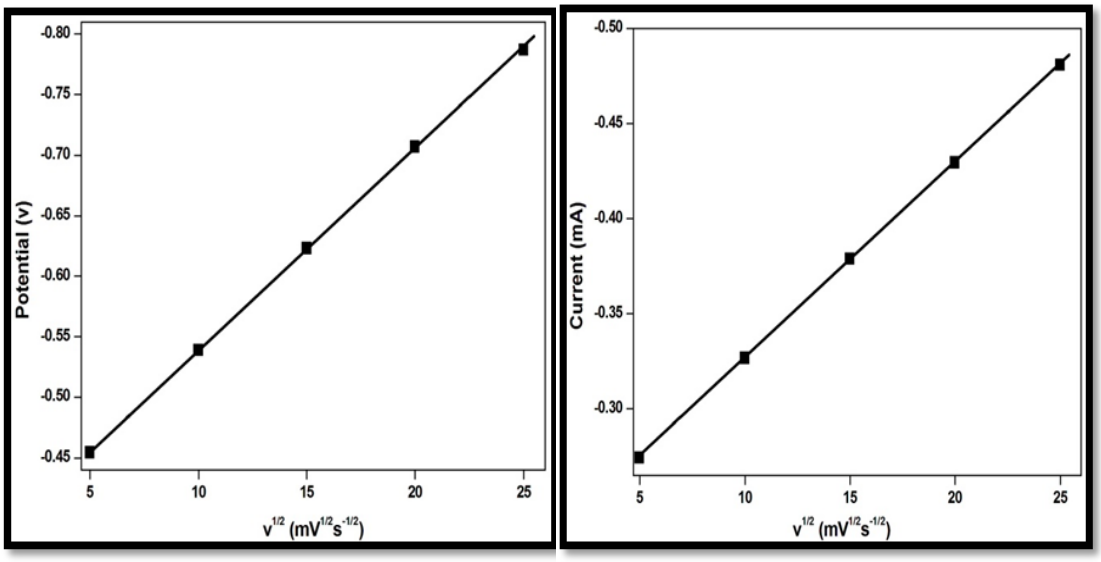

(f)

Figure.6.10. (a), (c), (e) Effect of scan rate on the redox current response for 220, 240 µM, 240 µM of ortho-, para- and meta-NP in 0.1 M PBS solution (b), (d) and (f) Linear relationship between E_{pa}, I_{pa} and square root of scan rate

The kinetic features of the synthesized 0.008 M molar ratio of rGONS/ β-CD/ZnO nanocomposite modified glassy carbon electrode towards the electrocatalytic reduction and oxidation of ortho-, para- and meta-nitrophenol isomers are examined using cyclic voltammerty by the effect of potential scan rate in the range from 10 mV/s

to 50 mV/s in 0.1 M PBS solution containing 220 µM of ortho-, 240 µM of para- and 240 µM of meta-nitrophenol isomers and the obtained results are presented in the Figure.6.10.(a, c and e). It is observed from the cyclic voltagramm of ortho-, para- and meta-nitrophenol isomers, the redox peak current is linear with the scan rate for the range from 10 to 50 mV/s and the increase in the scan rate revealed that the anodic and cathodic peak potential are shifted to the positive and negative values respectively, thereby evident that the electrocatalytic redox process of ortho-, para- and meta-nitrophenol isomers are reversible. The calibration graph is drawn for the square root of scan rate vs reduction peak potential and current and are as shown in the Figure.6.10.(b, d and f) for ortho-, para- and meta-NP respectively. It is observed from the calibration graph that the scan rate depends on the electrocatalytic reduction peak current of ortho-, para- and meta-nitrophenol isomers and increases linearly with the square root of the scan rate. This phenomenon illustrates that the electrochemical detection of ortho-, para- and meta-nitrophenol isomers are diffusion controlled reversible electrochemical redox process [41-43].

6.5.4. Effect of analyte (o-, p- and m-NP) concentration

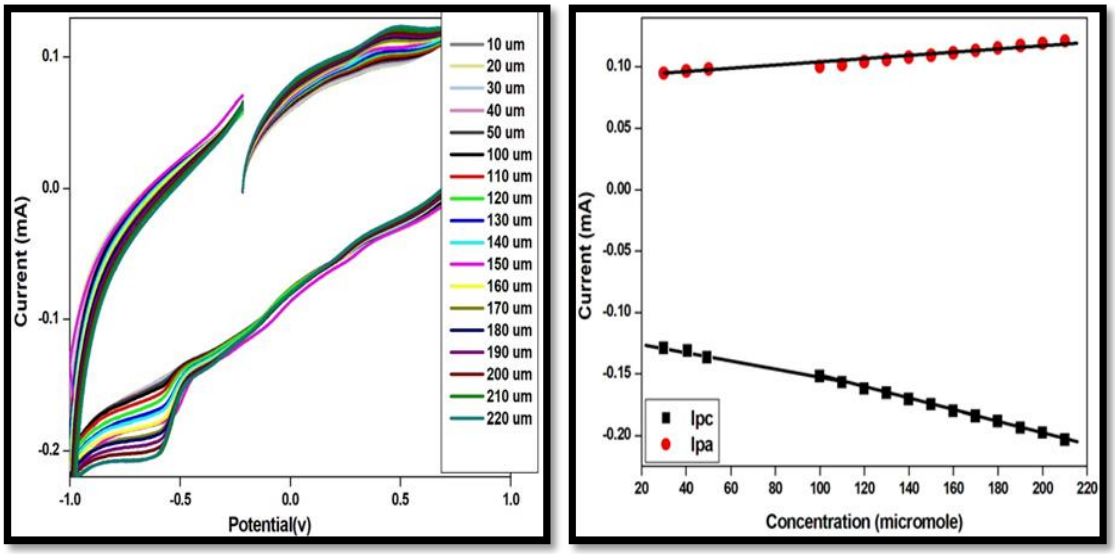

(a)

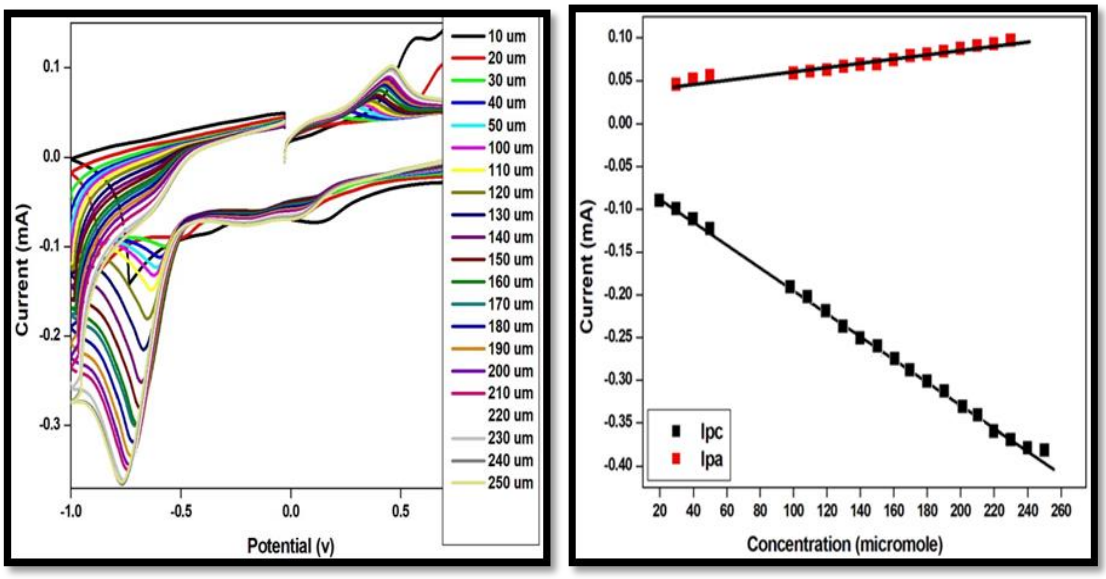

(b)

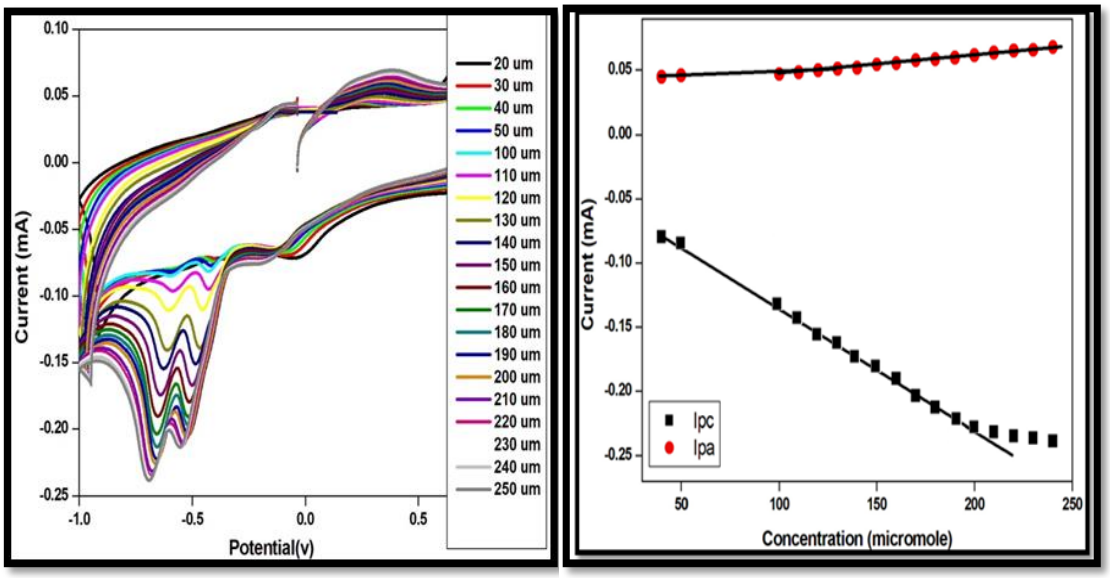

(c)

Figure.6.11. Cyclic voltagramm of rGONS/β-CD/ZnO/GCE in 0.1 M of PBS solution containing various concentrations of (a) o-NP, (b) p-NP and (c) m-NP

Figure.6.11.(a, b and c) shows the cyclic voltammetric response of various concentration of ortho-, para- and meta-nitrophenol isomers at the 0.008 M of rGONS/β-CD/ZnO modified glassy carbon electrode in 0.1 M of phosphate buffer solution (PBS) at the scan rate of 10 mV/s. The electrode potential is set between -1.0 V to +1.0 V. The cyclic voltagramm shows that the anodic and cathodic peak current of

ortho-, para- and meta-nitrophenol isomers increases gradually with the increase in the concentration from 10 μM to 210 μM, 10 μM to 240 μM and 20 μM to 240 μM, respectively. With the continuous addition of ortho-, para- and meta-NP isomers into the PBS solution leads to the decrease in the redox peak current, which indicates the saturation state of electrocatalytic detection capability of synthesized rGONS/ β-CD/ZnO nanocomposites. This phenomenon also indicates that the accumulation of o-, p- and m-NP sites onto the rGONS/β-CD/ZnO modified GCE electrode surface reaches the maximum concentration and thereby inhibits the electrocatalytic redox reaction. Figure.6.11.(a-c) shows the calibration graph of concentration dependent redox peak current of ortho-, para- and meta-nitrophenol isomers, respectively. From the calibration graph, the linear concentration ranges and sensitivitiy of ortho-, para- and meta-nitrophenol isomers are studied and the calculated values are tabulated in the Table.6.1.

Table.6.1. Linear range of detection and sensitivity value of the rGONS/β-CD/ZnO nanocomposite

Nitrophenol isomers	**Linear range of detection (μM)**	**Sensitivity ($mA\mu M^{-1}cm^{-2)}$**
Ortho-nitrophenol	20 to 210	4.7
Para-nitrophenol	20 to 240	13.8
Meta-nitrophenol	40 to 200	2.2

It is revealed from the results that the linear range of response and sensitivity of the synthesized rGONS/β-CD/ZnO modified GCE is found to be better for the detection of para-nitrophenol than the other nitrophenol isomers. Hence, the synthesized 0.008 M molar ratio of rGONS/β-CD/ZnO nanocomposite is a promising electrode modifying material for the electrochemical determination of para-nitrophenol

6.6. CONCLUSION

The various molar ratio of (0.002 M, 0.004 M, 0.006 M, 0.008 M and 0.01 M) rGONS/β-CD/ZnO nanocomposites are facilely synthesized by wet chemical method and employed as a novel electrode materials for the electrochemical detection of nitrophenol isomers (ortho-, para- and meta-nitrophenol). The XRD analysis revealed the wurtzite structure of zinc oxide nanoparticles and is embellished on the surface of rGO/β-CD nanosheets with the crystallite size in the range from 19 to 27 nm. SEM analysis showed the spindle like morphology and the variation in the spindle size could be due to the impact of molar ratio of Zn^{2+} ions on the surface of rGONS/β-CD/ZnO nanocomposites. The uniformly embellished spindle is observed for the 0.008 M molar ratio of Zn^{2+} ions in the reaction system. The HRTEM analysis also showed the uniform embellishment of spindle shaped zinc oxide nanoparticles on the surface of rGONS/ β-CD without agglomeration. The synthesized rGONS/β-CD/ZnO nanocomposites are deposited on the glassy carbon electrode to study the electrochemical performance towards the detection of nitrophenol isomers (o-, p- and m-NP) that showed the significant improvement in the electrical conductivity and electrocatalytic activity in comparison with that of rGONS/ZnO nanocomposite modified GCE. The effect of rGONS/β-CD/ZnO nanocomposite concentrations (0.002 M, 0.004 M, 0.006 M, 0.008 M and 0.01 M) modified GCE electrode are also investigated and the results showed that the rGONS/β-CD/ZnO nanocomposite with 0.008 M molar ratio of zinc acetate dihydrate has the highest electrochemical signal towards the detection of ortho-nitrophenol. This may be due to the presence of uniformly embellished smaller sized spindle like ZnO nanoparticles on the surface of rGO/β-CD nanosheets as evidenced from XRD and SEM analysis. The as prepared 0.008 M molar ratio of rGONS/ β-CD/ZnO nanocomposite modified GCE is employed for the electrochemical detection of o-, p- and m-nitrophenol which exhibited an excellent performance with the linear range of detection from 20 to 210 μM, 20 to 240 μM and 40 to 200 μM respectively. The sensitivity values of rGONS/β-CD/ZnO nanocomposite towards the detection of o-, p- and m-nitrophenols are found to be 4.7 mA μM^{-1} cm^{-2}, 13.8 mA μM^{-1} cm^{-2} and 2.2 mA μM^{-1} cm^{-2} respectively. It is revealed from the voltammetric analysis that the synthesized rGONS/β-CD/ZnO nanocomposite is best suited for the detection of para-nitrophenol isomer.

References

1. H. Wang, S. Yao, Y. Liu, S. Wei, J. Su, G. Hu, A novel electrochemical sensor based on flower shaped zinc oxide nanoparticles for the effiecient detection of dopamine, Biosens. Bioelectron, 87, 417-421, (2017).

2. S.E.F. Kleijn, S.C.S. Lai, M.T.M. Koper, P R. Unwin, Angew. Chem. Int. Ed, 53, 3558-3586, (2014).

3. X. Luo, A. Morrin, A. J. Killard and M. R. Smyth, Applicatio of nanoparticles in electrochemical sensors and biosensors, Electroanalysis, 18, 319-326, (2006).

4. W. Yang, K. R. Ratinac, S. P. Ringer, P. Thordarson, J. J. Gooding and F. Braet, Angew. Chem. Int. Ed, 49, 2114-2138, (2010).

5. Yu, Z. Liang, J. Cho and F. Caruso, Nanostructured electrochemical sensor based on dense gold nanoparticles films, Nano Lett, 3, 1203-1207, (2003).

6. J.S. Jang, W.T. Koo, S.J. Choi and I.D. Kim, Synthesis of sulfones and sulphonamides via sulfinate anions: revisiting the utility of thiosulfonates, J. Am. Chem. Soc, 139, 11868-11876, (2017).

7. P.K. Kannan, D.J. Late, H.Morgan, C.S. Rout, Recent development in 2D layered inorganic nanomaterials for sensing, Nanoscale, 7, 13293-13312, (2015).

8. Y. Li, W. Luo, N. Qin, J. Dong, J. Wei, W. Li, S. Feng, J. Chen, J. Xu, A.A. Elzatahry, M.H. Es Saheb, Y. Deng, D. Zhao, Angew. Chem. Int. Ed, 53, 9035-9040, (2014).

9. Stassen, N. Burtch, A. Talin, P. Falcaro, M. Allendorf, R. Ameloot, An updated road map for the investigation of metal organic frameworks with electronic devices and chemical sensors, Chem. Soc. Rev, 46, 3185-3241, (2017).

10. C.H. Chen, S.J. Chang, S.P. Chang, M.J. Li, I.C. Chen, T.J. Hsueh, C.L. Hsu, Novel fabrication of UV photodetector based on ZnO nanowire/p-GaN heterojunctio, Chem. Phys. Lett, 476, 69-72, (2009).

11. Ghanbari, M. Moloudi, Fabrication and characterization of nano-enzymatic glucose sensor based on ternary NiO/CuO/Polyaniline nanocomposite, Anal. Biochem, 512, 91-102, (2016).

12. S.H. Liao, H.J. Jhuo, P.N. Yeh, Y.S. Cheng, Y.L. Li, Y.H. Lee, S. Sharma, S.A. Chen, Fullerene derivative doped zinc oxide nanofilm as the cathode of inverted polymer solar cells with low band gap polymer (PTB7-Th) for high performance, Adv.Mater, 4, (2013).

13. C. Wang, J. Du, H. Wang, C.E. Zou, F. Jiang, P. Yang, Y. Du, Sens. Actuators, B, 204, 302-309, (2014).

14. X. Zhu, I. Yuri, X. Gan, I. Suzuki, G. Li, Biosens. Bioelectron, 22, 1600-1604, (2007).

15. Deepak Balram, Kuang Yow Lian, Neethu Sebastian, A novel electrochemical sensor based on flower shaped zinc oxide nanoparticles for the efficient detection of dopamine, Int. J. Electrochem. Sci, 13, 1542-1555, (2018).

16. C. S. Rout, S. Hari Krishna, S.R.C. Vivekchand, A. Govindaraj and C.N.R. Rao, Inorganic nanowires: Applications, properties, and characterization, Chem. Phys. Lett, 418, 586-590, (2006).

17. L.J. Bie, X.N. Yan, J. Yin, Y.Q. Duan, Z.H. Yuan, Sens. Actuators, B, 126, 604-608, (2007).

18. G. Sberveglieri, C. Baratto, E. Comini, G. Faglia, M. Ferroni, A. Ponzoni, A. Vomiero, Synthesis and characterization of semiconducting nanowires, Sens. Actuators, B, 121, 208-213, (2007).

19. C. Ge, Z. Bai, M. Hu, D. Zeng, S. Cai, C. Xie, Mater. Lett, 62, 2307-2310, (2008).

20. T. Gao, T.H. Wang, Synthesis and properties of multipod-shaped ZnO nanorods for gas-sensor applications, Appl. Phys. A, 80, 1451-1454, (2005).

21. O. Lupan, L. Chow, S. Shishiyanu, E. Monaico, T. Shishiyanu, V. Şontea, B. Roldan Cuenya, A. Naitabdi, S. Park and A. Schulte, Mater Res Bull, 44, 63-69, (2009).

22. A. Nemeth, E. Horvath, Z. Labadi, L. Fedak, I. Barsony, Sens. Actuators, B, 127, 157-160, (2007).

23. V. Ramalakshmi, J. Balavijayalakshmi, Investigation on embellishment of metal nanoparticles on graphene nanosheets and its sensing applications, Mechanics, Materials Science & Engineering. 14, 1-14, (2018).

24. Jaewon Hwang, Taeshik Yoon, Sung Hwan Jin, Jinsup Lee, Taek-Soo Kim, Soon Hyung Hong, Seokwoo Jeon, Enhanced mechanical properties of graphene/copper nanocomposites using a molecular-level mixing process, Adv. Mater, 25, 6724-6729, (2013).

25. Y. Guo, S. Guo, J. Ren, Y. Zhai, S. Dong, E. Wang, Cyclodextrin functionalized graphene nanosheets with high supramolecular recognition capability: synthesis and host-guest inclusion for enhanced electrochemical performance, ACS Nano, 4, 4001-4010, (2010).

26. M. Chen, Y. Meng, W. Zhang, J. Zhou, J. Xie, G. Diao, β-Cyclodextrin polymer functionalized reduced-graphene oxide: Application for electrochemical determination imidacloprid, Electrochimical Acta, 108, 1-9, (2013).

27. Rajkumar Devasenathipathy, Shin-Hung Tsai, Shen-Ming Chen, Chelladurai Karuppiah, Raj Karthik, Sea Fue Wang, Electrochemical synthesis of β-Cyclodextrin functionalized silver nanoparticles and reduced graphene oxide composite for the determination of hydrazine, Electroanalysis. 28, 1-8, (2016).

28. Dipanwita Majumdar, Sonochemically synthesized beta-cyclodextrin functionalized graphene oxide and its efficient role in adsorption of water soluble brilliant green dye, J. Environ Anal Toxicol, 6, (2016).

29. Shanshan Wang, Yang Li, Xiaobin Fan, Fengbao Zhang, Guoliang Zhang, β-Cyclodextrin functionalized graphene oxide: an efficient and recyclable

adsorbent for the removal of dye pollutants, Front. Chem. Sci. Eng, 9, 77-83, (2014).

30. Murugan Saranya, Rajendran Ramachandran, Fei Wang, Graphene-zinc oxide (G-ZnO) nanocomposite for electrochemical supercapacitor applications, Journal of Science: Advanced Materials and Devices, 1, 454-460, (2016).

31. Kuo Yuan Hwa, Boopathi Subramani, Synthesis of zinc oxide nanoparticles on graphene-carbon nanotube hybrid for glucose biosensor applications, Biosensors and Bioelectronics, 62, 127-133, (2014).

32. Qi Zhang, Zhong Wu, Chen Xu, Lei Liu, Wenbin Hu, Temperature-driven growth of reduced graphene oxide/copper nanocomposites for glucose sensing. 27, 495603, (2016).

33. Junwei Ding, Shiying Zhu, Tao Zhu, Wei Sun, Qing Li, Gang Wei, Zhiqiang Su, Hydrothermal synthesis of zinc oxide-reduced graphene oxide nanocomposites for an electrochemical hydrazine sensor, RSC Adv, 5, 22935-22942, (2015).

34. S. K. Shahenoor Basha, K. Vijay Kumar, G. Sunita Sundari, M. C. Rao, Structural and electrical properties of graphene oxide-doped PVA/PVP blend nanocomposite polymer films, Advances in Materials Science and Engineering. 4372365, 1-11, (2018).

35. Kuo Yuan Hwa, Boopathi Subramani, Synthesis of zinc oxide nanoparticles on graphene-caarbon nanotube hybrid for glucose biosensor applications Biosensors and Bioelectronics, 62, 127-133, (2014).

36. Harish kumar, Manisha Kumari, Synthesis, characterization, and antibacterial study of zinc oxide-graphene nanocomposites, Asian. J. Pharm. Clin. Res, 10, 206-209, (2017).

37. Xuan Zhang, Yi Chi Zhang, Li Xia Ma, One-pot facile fabrication of graphene-zinc oxide composite and its enhanced sensitivity for simultaneous electrochemical detection of ascorbic acid, dopamine and uric acid, Sensors and Actuators B, 227, 488-496, (2016).

38. Ting Hu, Lie Chen, Kai Yuan, Yiwang Chen, Poly (N-vinylpyrrolidone)-decorated reduced graphene oxide with ZnO grown in situ as a cathode buffer layer for polymer solar cells, Chem. Eur. J, 20, 17178-1718, (2014).

39. Lin Guo, Shihe Yang, Synthesis and characterization of poly (vinylpyrrolidone)-modified zinc oxide nanoparticles, Chem. Mater, 12, 2268-2274, (2000).

40. Weilu Liu, Cong Li, Yue Gu, Liu Tang, Zhiquan Zhang, Ming Yang, One-step synthesis of β-cyclodextrin functionalized graphene/Ag nanocomposite and its application in sensitive determination of 4-nitrophenol, Electroanalysis, 25, 1-10, (2013).

41. Tanvir Arfin, Rani Bushra, Faruq Mohammad, Electrochemical sensor for the sensitive detection of o-nitrophenol using graphene oxide-poly (ethyleneimine) dendrimer-modified glassy carbon electrode, Graphene Technol, 21, 1-15.

42. Ehab Salih, Moataz Mekawy, Y.A. Rabeay, Hassan, M. Ibrahim El Sherbiny, Synthesis, characterization and electrochemical-sensor applications of zinc oxide/graphene oxide nanocomposite, J. Nanostruct Chem, 6, 137-144, (2016).

43. Yanhong Xu, Yulong Wang, Yaping Ding, Liqiang Luo, Xiaojuan Liu, Yunxiao Zhang, Determination of p-nitrophenol on carbon paste electrode modified with a nanoscaled compound oxide Mg(Ni)FeO, Appl. Electrochem, 43, 679-687, (2013).

44. Yang Yun, Electrochemical Sensor for Ultrasensitive determination of bisphenol a based on gold nanoparticles/β-cyclodextrin functionalized reduced graphene oxide, Int. J. Electrochem. Sci, 11, 2778-2789, (2016).